

estimate $(g''/2\pi) = 130 \pm 40 \text{ MHz } \text{\AA}^{-2}$. From this, we predict that the anomaly in specific heat in hcp ^3He should be observable below about $T \approx 0.005\Theta_0$ at molar volumes of about 19 cm^3 .

It should be noted that a Hamiltonian of the form (6) does not contribute to the zero-field susceptibility at high T . The bcc phase of solid ^3He exhibits an anomaly in the NMR measurements^{10,11} also. The spectral function for the transverse relaxation is quite distinctly not a Gaussian, as is expected approximately for an exchange-narrowed line. On a preliminary examination, we find that indirect spin interactions may be responsible for this anomaly. We intend to explore this matter further as well as other consequences of indirect spin interactions including their effect on thermal conductivity.

I wish gratefully to acknowledge discussions with Professor H. Suhl, Dr. W. F. Brinkman, Dr. N. R. Werthamer, and Dr. C. Herring.

¹E. C. Héltemes and C. A. Swenson, Phys. Rev. 128,

1512 (1962).

²H. H. Sample and C. A. Swenson, Phys. Rev. 158, 188 (1967).

³R. C. Pandorf and D. O. Edwards, Phys. Rev. 169, 222 (1968).

⁴P. N. Henriksen, M. F. Panczyk, S. B. Trickey, and E. D. Adams, Phys. Rev. Letters 23, 518 (1969).

⁵D. J. Thouless, Proc. Phys. Soc. (London) 86, 893 (1965).

⁶L. H. Nosanow and C. M. Varma, Phys. Rev. Letters 20, 912 (1968), and Phys. Rev. 187, 660 (1969).

⁷C. M. Varma and L. H. Nosanow, Phys. Rev. (to be published).

⁸The coefficients g_{jj}' should not be identified with derivatives of J_{jj} with respect to equilibrium interparticle separation. This point has been stressed in Ref. 7 and in R. P. Giffard, thesis, Oxford University, 1968 (unpublished).

⁹M. G. Richards, J. Hatton, and R. P. Giffard, Phys. Rev. 139, A91 (1965).

¹⁰R. C. Richardson, A. Landesman, E. Hunt, and H. Meyer, Phys. Rev. 146, 244 (1966).

¹¹M. G. Richards, talk delivered at the Quantum Crystal Conference, Aspen, Colorado, 1969 (unpublished).

OBSERVATION OF COLLISIONLESS ELECTROSTATIC SHOCKS*

R. J. Taylor, D. R. Baker, and H. Ikezi†

Department of Physics, University of California, Los Angeles, California 90024

(Received 19 December 1969)

Large-amplitude ion-acoustic waves ($e\phi/kT_e \lesssim 0.3$) are excited in the University of California, Los Angeles double-plasma device by the interpenetration of two plasmas with high electron-to-ion temperature ratios ($6 < T_e/T_i < 20$). A compressional wave with a ramp shape is found to steepen in a fashion consistent with the classical overtaking predicted by the usual Riemann invariants. This steepening continues until dispersive short scale ($k \approx \frac{1}{2}k_D$) oscillations develop at the front. Ions streaming in front of the shock are also observed.

Moiseev and Sagdeev¹ and Montgomery² have shown that, in the limit $T_e/T_i \gg 1$, the development of a finite-amplitude ion-acoustic wave is given by a Riemann solution which results in a steepening of the ion waves into a shock-like front. Andersen et al.³ have reported observation of steepening of ion-acoustic waves in a Q device. Their shock thickness was determined by the ion-ion collision distance and was more than 1000 Debye lengths λ_D .

Here we wish to report the observation of a magnetic-field-free collisionless shock formation with a thickness of about $5\lambda_D$. These shocks are excited by either a step or a ramp voltage applied between two plasmas (the driver and the target). Steepening is observed (of course) only for the ramp initial condition.

The two plasmas are produced in the University of California, Los Angeles double-plasma device⁴ by electron bombardment of argon at about 5×10^{-4} Torr in two identical chambers, placed end to end, which are insulated from each other and separated by a negatively biased grid, held at a fixed potential. The grid isolates the electrons in one plasma from those of the other. The chamber dimensions are length = diam = 30 cm = $1000\lambda_D$. Ion-ion collisions are unimportant since typical densities are 10^9 cm^{-3} with ion temperature about 0.2 eV ($\lambda_{De} > 10^3\lambda_D$). The ion-neutral collision effects can also be ignored. The mean free path for charge transfer is greater than $300\lambda_D$.

Our wave excitation mechanism is different from the well-known grid excitation.⁵ Although

we use a grid between the plasmas, its function is to allow the maintenance of a significant gradient in the electron densities in the vicinity of the grid. Therefore the electrons are prevented from short-circuiting potential differences between the target and driver plasmas.

The excitation of a ramp wave in our system is accomplished as follows. First the driver plasma density is adjusted to be higher than that of the target plasma [as shown in Fig. 1(a)] by suitable choices of filament emission and electron-bombarding energy of the background neutral gas. During this process wave propagation is inhibited by holding the driver plasma ions at a slightly negative potential with respect to the target plasma. Then at $t=0$ a ramp potential [Fig. 1(b)] is applied to the driver plasma. The maximum value ϕ_A of this potential determines the wave potential; about half of the applied potential drives a compression and the other half a rarefaction wave into the target and driver plasmas, respectively. Both the amplitude ϕ_A and the rise time τ of the ramp can be varied. When τ has its minimum value ($0.1 \mu\text{sec}$) we get the special case of a "step."

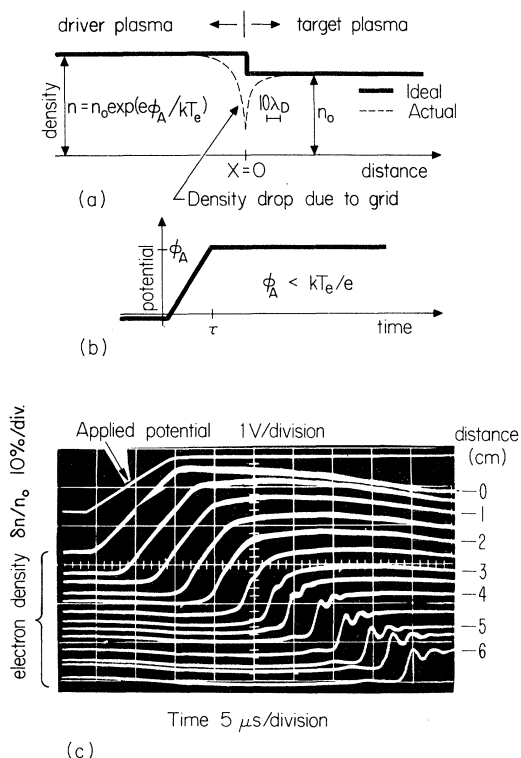


FIG. 1. (a) Initial plasma density profile. (b) Potential applied between the two plasmas at the time of wave launching. (c) Plot of electron density versus time with distance as parameter. $n_0=10^9 \text{ cm}^{-3}$, initial density rise = 25%, $T_e=1.5 \text{ eV}$, $T_i=0.2 \text{ eV}$.

Figure 1(c) shows the nature of the compression-wave propagation due to the applied potential ramp shown on the top trace. As the wave propagates it steepens, followed by short-scale oscillations resembling a wave train⁶ with a frequency about $0.5\omega_{pi}$.⁷ The Riemann solution,² which neglects both dissipation and dispersion, exhibits steepening in a time

$$t_s = \tau n_0 / \delta n$$

where τ is the time duration of the initial density ramp and $\delta n/n_0$ is the normalized density perturbation. The data of Fig. 1(c) agree with this prediction within 30%.

In front of the shock a small precursor can be seen. Using an ion-energy analyzer,^{8,9} we have found this to be a group of streaming ions, causing a double-humped ion distribution. Some of the ions come from the driver plasma, and some, originally part of the target plasma, are accelerated by the front, i.e., reflected by the front when viewed in the shock rest frame. The number of ions streaming in front of the shock is found to depend on the excited wave potential and the T_e/T_i ratio. Computer experiments by Mason¹⁰ show a similar ion stream. Figure 2 shows the change in shock propagation when the T_e/T_i ratio is

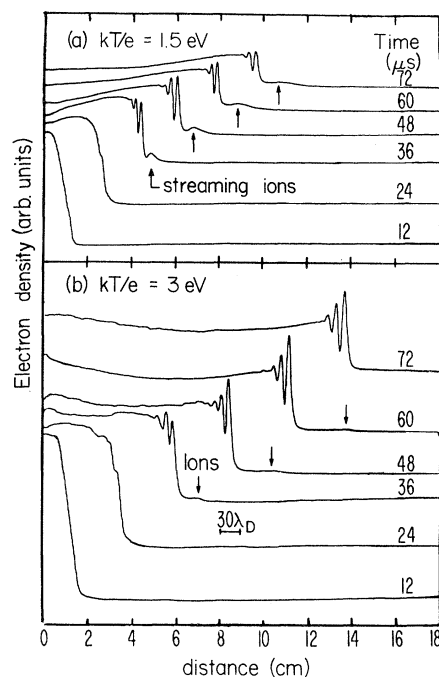


FIG. 2. Spatial plot of the shock propagation at (a) lower and (b) higher electron temperatures, showing variation in the amount of streaming ions. $T_i=0.2 \text{ eV}$; $n_0=10^9 \text{ cm}^{-3}$; initial $\delta n/n_0=25\%$; excitation (a) 1 V, (b) 2 V.

changed by a factor of 2. These plots (in which the abscissa is axial position at various fixed times, i.e., the opposite of the case in Fig. 1) are obtained by sampling the saturated electron current¹¹ from a Langmuir probe at a fixed time, as indicated, while sweeping the probe position axially. Lower T_e , as shown in Fig. 2(a), results in an increase in the number of the streaming ions. The streaming ions appear to dampen the shock energy. At higher T_e [Fig. 2(b)] a smaller ion stream is excited since the wave propagates faster, there is less damping, and a longer wave train is observed. In these shock waves the measurement of electron density shows a dependence $n_e \approx n_0 \exp(e\phi/T_e)$.

For a high T_e/T_i ratio the linear and nonlinear ion-acoustic wave behavior can be described (neglecting reflected ions) by the fluid equations. In that limit Washimi and Taniuti¹² have shown that the solution to the linearized piston problem (in our case this is a step excitation) for large t can be given in terms of the integrated Airy function with argument $(\frac{2}{3})^{1/3}(\lambda_D/x)^{1/3}(x-C_s t)/\lambda_D$, where $C_s = (kT_e/M)^{1/2}$ is the ion-acoustic speed. In Fig. 3, we show the spatial ion-acoustic wave response at a fixed time due to step excitations ($\tau > 1/\omega_{pi}$) of different amplitudes. For small amplitude (top trace) an Airy-function-type response results.

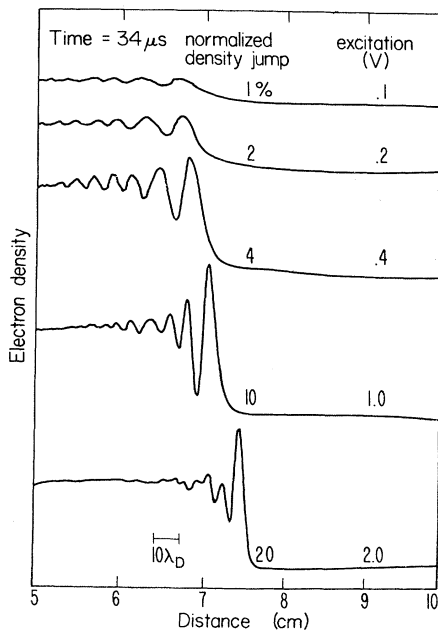


FIG. 3. Plasma response to a potential-step excitation, showing an Airy-type structure at small amplitudes. $T_e = 4$ eV, $T_i = 0.2$ eV, $n_0 = 10^9$ cm⁻³. Time is fixed at 34 μ sec after the step excitation.

The first two peaks in the wave train are separated by about $12\lambda_D$. A table of the integrated Airy function shows a separation between the corresponding two peaks equal to $16\lambda_D$. This is a good agreement considering the uncertainties in the measured plasma density. As the excitation amplitude is increased, the wave train and the shock front shift to the right (i.e., the Mach number increases) and the shock transition region shortens. At the same time the wave number of the wave train shows a considerable increase, in agreement with the predictions of Moiseev and Sagdeev.¹ Thus, the Airy structure, which is a linear result for a boundary-value problem, is modified at Mach numbers > 1 . At Mach numbers about 1.2 (maximum produced) the wave train is reduced to less than 3 oscillations indicating increase in dissipation.¹³ We have found the dependence of the Mach number on the density jump to be $M = 1 + (0.75 \pm 0.2)\delta n/n_0$, valid up to our maximum $\delta n/n_0$ (< 0.3).

We wish to express our thanks for assistance given by Professor K. R. MacKenzie and Professor A. Y. Wong, and for helpful discussions with B. D. Fried (who suggested the use of the ramp excitation) and C. F. Kennel.

*Research supported in part by the U. S. Atomic Energy Commission.

†On leave from Institute of Plasma Physics, Nagoya University, Nagoya, Japan.

¹S. S. Moiseev and R. Z. Sagdeev, *J. Nucl. Energy*, Pt. C **5**, 43 (1963).

²D. Montgomery, *Phys. Rev. Letters* **19**, 1465 (1967).

³H. K. Andersen, N. D'Angelo, P. Michelsen, and P. Nielsen, *Phys. Fluids* **11**, 606 (1968).

⁴R. J. Taylor, H. Ikezi, and K. R. MacKenzie, in *Proceeding of the International Conference on Physics of Quiescent Plasmas*, Paris, September 1968 (to be published).

⁵A. Y. Wong, R. W. Motley, and N. D'Angelo, *Phys. Rev.* **133**, A436 (1964).

⁶C. F. Kennel and R. Z. Sagdeev, *J. Geophys. Res.* **72**, 3303 (1967).

⁷S. G. Alikhanov, V. G. Belan, and R. Z. Sagdeev, *Zh. Eksperim. i Teor. Fiz. - Pis'ma Redakt.* **7**, 405 (1968) [*JETP Letters* **7**, 318 (1968)].

⁸H. Ikezi and R. J. Taylor, *Phys. Rev. Letters* **22**, 923 (1969).

⁹H. Ikezi and R. J. Taylor, to be published.

¹⁰R. J. Mason, *Bull. Am. Phys. Soc.* **14**, 1043 (1968).

¹¹In order to display these short-scale oscillations the electron saturation current was used because the ion saturation current response is poor at ω_{pi} due to a large ion sheath and the presence of a displacement current. We have checked that in this plasma electron

collection itself did not cause the observed oscillations near ω_{pl} : (1) The wave train did not change with change in positive bias of the probe; (2) exciting the probe with a potential step caused no oscillations in

the electron current.

¹²H. Washimi and T. Taniuti, Phys. Rev. Letters **17**, 996 (1966).

¹³F. V. Coroniti, private communication.

ELECTRIC-FIELD-INDUCED COLOR CHANGES AND PITCH DILATION IN CHOLESTERIC LIQUID CRYSTALS

Frederic J. Kahn*

Central Research Laboratories, Nippon Electric Co., Ltd., Kawasaki, Japan

(Received 1 December 1969)

A new electric-field-induced color range, in which colors change from blue to red with increasing field, has been observed in cholesteric liquid crystals. Observations of this new color range quantitatively confirm the theories of Meyer and de Gennes and enable identification of the specific nature of the electric-field-induced cholesteric-nematic phase transitions previously observed by other workers.

Introduction.—The dramatic color changes resulting from the application of electric fields to cholesteric liquid crystals have been well known since the initial investigations of Ferguson and Harper.¹ However a theoretical basis for these effects has yet to be quantitatively confirmed.

Recently Meyer² and de Gennes³ calculated the effects of external electric² and magnetic^{2,3} fields on the helical structure of cholesteric materials. For the magnetic field case their predictions have been verified by the experiments of Durand et al.⁴ and Meyer.⁵ Although the electric-field-induced cholesteric-nematic phase transitions predicted by Meyer have been observed by Wysocki, Adams, and Haas⁶ and by Baessler and Labes,⁷ until the current investigation, the specific nature of these experimentally observed transitions has remained uncertain.⁸

We report here the observation of a new electric-field-induced color range, different from that reported by Harper and other previous workers. In this new color range, colors change from blue to red with increasing electric field for fields applied normal to the helical-ordering axes. In contrast, the effects observed by Harper change from red to blue with increasing field and have been generally attributed to fields applied parallel to the helical-ordering axes.¹ The new color-change region enables us to observe the details of the cholesteric-nematic pretransition phenomena and thereby to identify the specific nature of this phase transition. These observations quantitatively confirm the theories of Meyer and de Gennes for the influence of electric fields applied normal to the helical-ordering axes.

Also reported here are observations of electric-field-induced 90° reorientations of the helical-ordering axes. Finally, certain transient phenomena are briefly considered.

Sample preparation.—The mixed crystal system composed of cholesteryl chloride (CC), cholesteryl nonanoate (CN), and cholesteryl oleyl carbonate (COC) was chosen for this investigation because it orders cholesterically at room temperature, at which all measurements were made, with a convenient range of pitches determined by the relative concentrations of the individual components. All component materials were obtained commercially and used without further purification.⁹ Three samples (I, II, III) with zero-field pitches $p_0 \approx (2330, 3400, 7400 \text{ \AA})$ and consisting by weight of CC (30.0, 37.5, 48.05%), CN (28.0, 25.0, 20.9%), COC (42.0, 37.5, 31.05%) were prepared by heating the materials to 90°C, mixing them mechanically without solvent, and allowing them to cool slowly to room temperature.

Fields were applied to the samples by sandwiching them between transparent electrodes of SnO₂ deposited on glass and separated by a 6- μ -thick Mylar spacer with a 5-mm-square window cut for the sample. The sample package was given mechanical stability by clamping with alligator clips. Typical sample resistivities were on the order of $10^{13} \Omega \text{ cm}$. Because of uncertainty in the actual sample thickness as a result of material viscosity and small deformations of the cut edges of the Mylar spacer, the quoted field values should be regarded as only approximate. However, because our principal results are independent of sample thickness, more precise

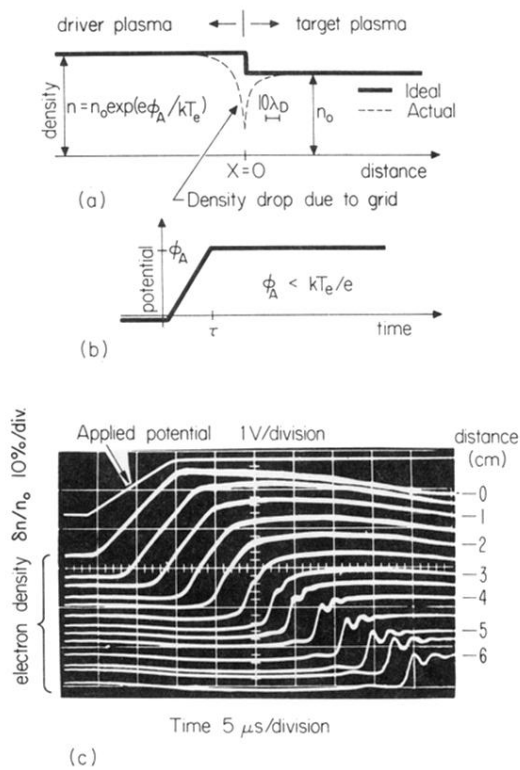


FIG. 1. (a) Initial plasma density profile. (b) Potential applied between the two plasmas at the time of wave launching. (c) Plot of electron density versus time with distance as parameter. $n_0 = 10^9 \text{ cm}^{-3}$, initial density rise = 25%, $T_e = 1.5 \text{ eV}$, $T_i = 0.2 \text{ eV}$.